

Supplemental Materials

Molecular Biology of the Cell

Champion et al.

Supplemental Figures

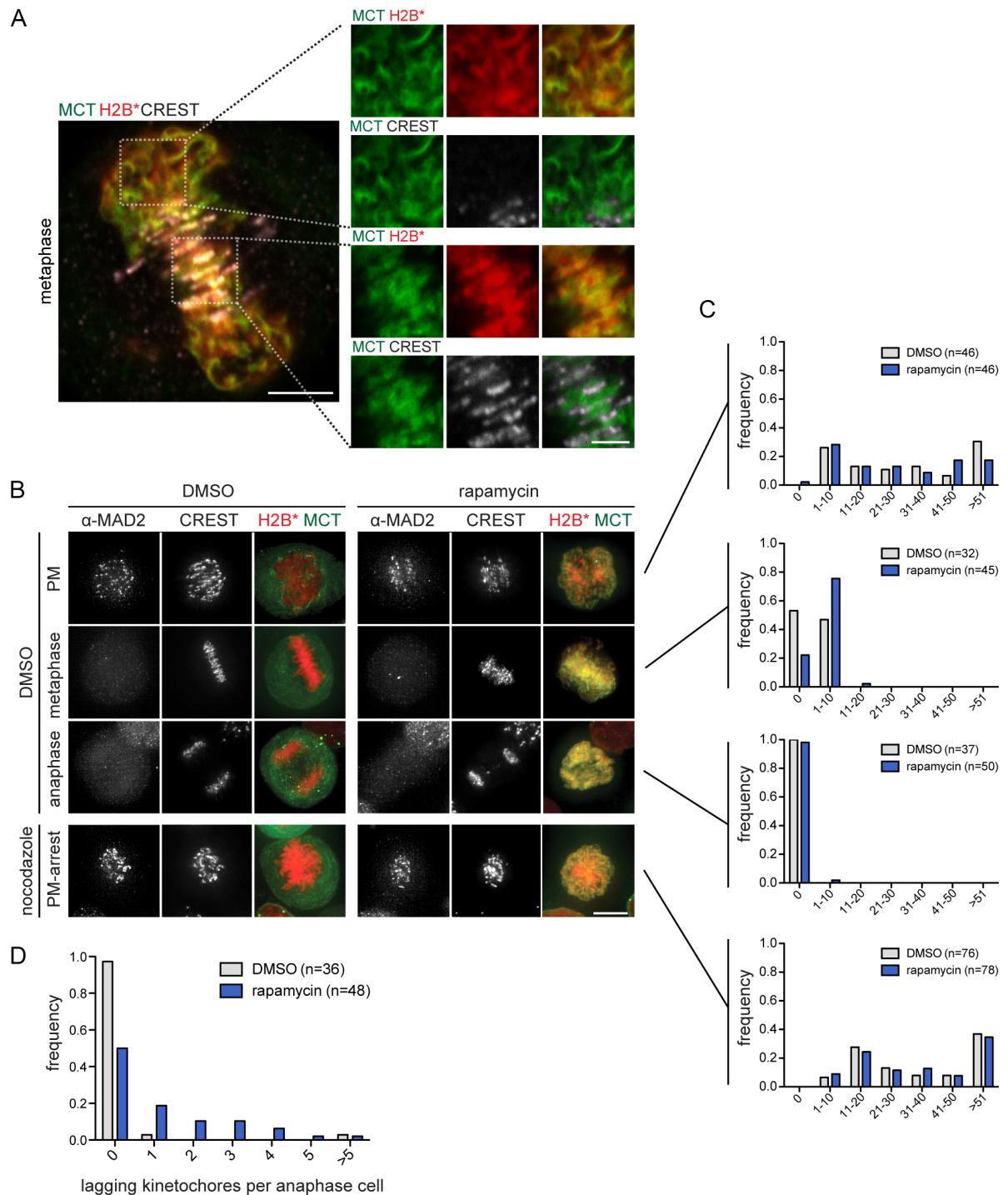


Figure S1. Kinetochores-MT attachments are not severely affected by persistent membrane-chromatin association in mitosis. (A) Representative close-up view of a synchronized MCT/H2B* cell stained for kinetochores (CREST) during metaphase in presence of rapamycin. Left panel bar, 5 μ m; Bar for zoomed images, 2.5 μ m. (B) Immunofluorescence (IF) analysis of MAD2 and kinetochores (CREST) in synchronized MCT/H2B* cells (as in A) treated with either DMSO or 100 ng/ml nocodazole before mitotic entry. (C) Quantification of the number of MAD2-positive kinetochores per cells at the indicated mitotic stage (N=2; n, number of analyzed cells). (D) Quantification of the number of lagging kinetochores in anaphase cells (N=2; n, number of cells). PM: prometaphase. Bars, 10 μ m.

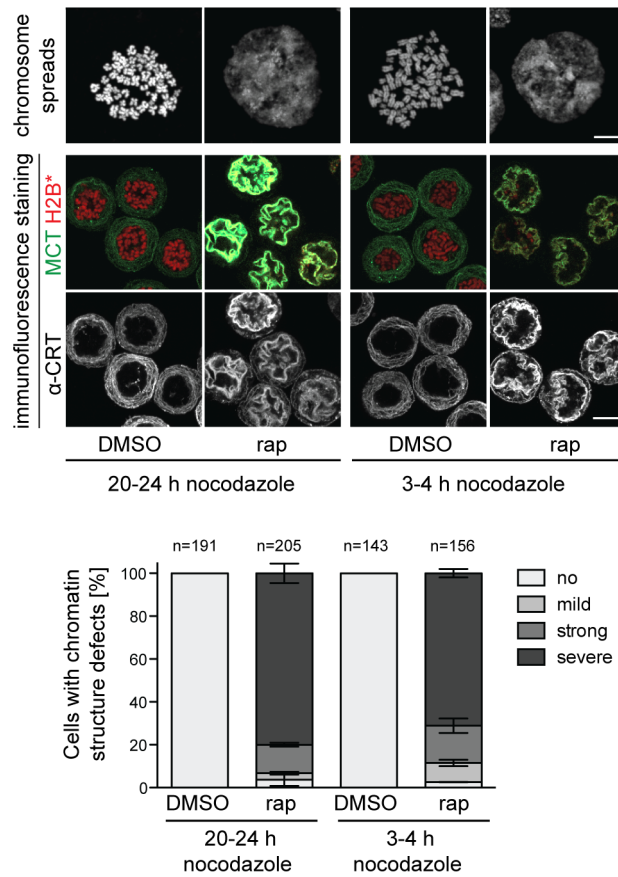


Figure S2. Analysis of mitotic chromosome spreads in MCT/H2B* cells. Quantitative analysis of mitotic chromatin organization for different time spans of nocodazole exposure, similar to Figure 4D. Below: Representative images of mitotic chromatin spreads (DNA, Hoechst), membrane organization (calreticulin (CRT) immunofluorescence), chromatin (mPlum on H2B) and MCT localization (GFP) from nocodazole-arrested MCT/H2B* cells. Bar, 10 μ m.

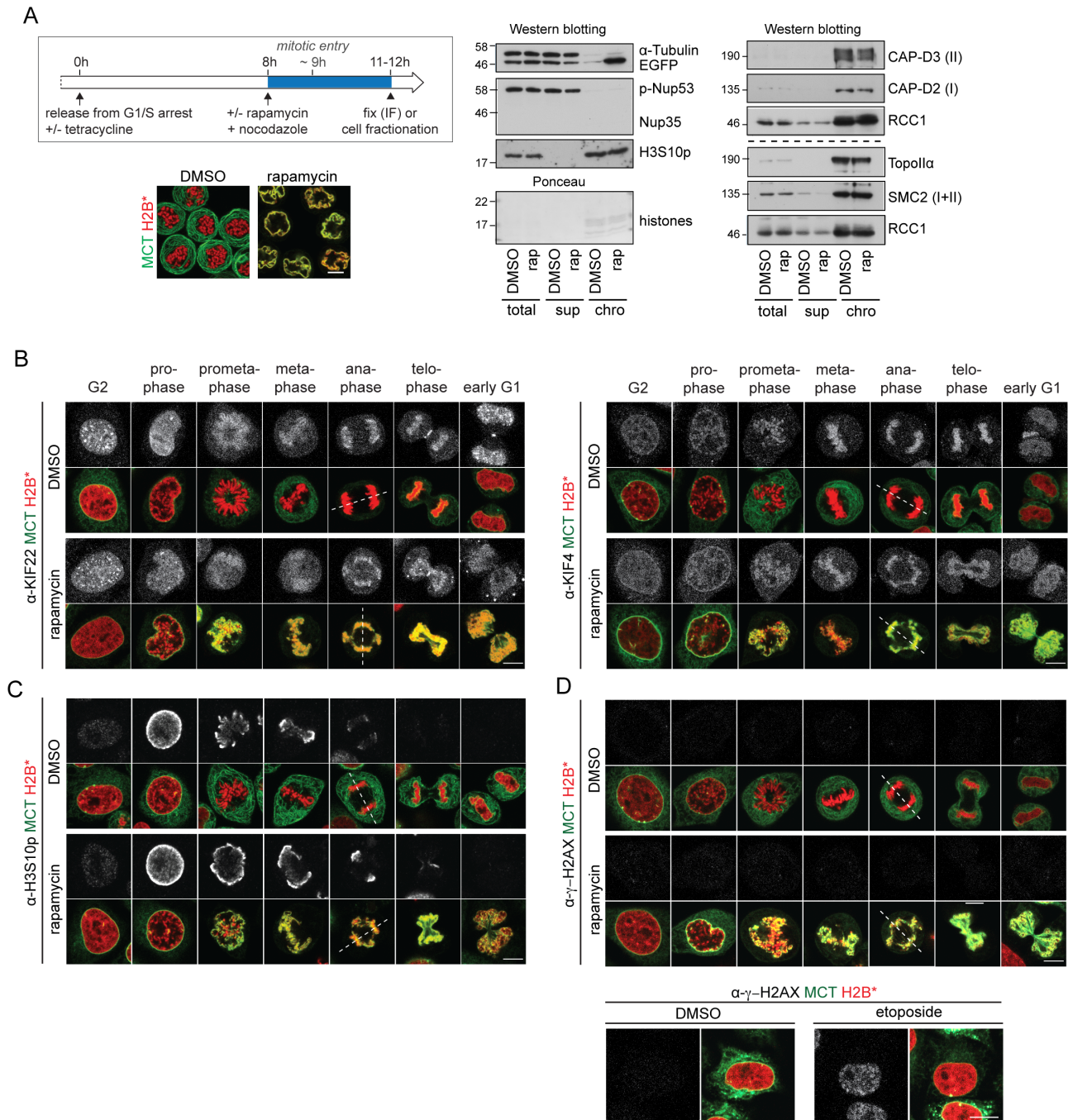


Figure S3. Chromatin condensation regulators can be efficiently loaded on mitotic chromatin in presence of the MCT. (A) Flowchart of the cell synchronization protocol combined with drug treatment. Representative confocal images of nocodazole-arrested, monoclonal MCT/H2B* cells arrested in mitosis. Biochemical fractionation of DMSO or rapamycin-treated mitotic MCT/H2B* cells. Immunoblot analysis of total cell extract (total), the soluble (supernatant (sup)) and chromatin-associated (chro) fractions using the indicated antibodies. The immunoblot on the left demonstrates proper cell fractionation (phosphorylated Nup53 and tubulin are found in the soluble fraction; phosphorylated H3S10 in the chromatin fraction). The immunoblot on the right shows that topoisomerase II α , condensin I (SMC2, CAP-D2) and condensin II (SMC2, CAP-D3) are efficiently retrieved in the chromatin fraction in rapamycin-treated MCT/H2B* cells. Load in the chromatin fractions corresponds to ten times the load in the total and cytoplasmic fractions. MCT/H2B* cells were treated as outlined in Figure 1B, immunostained using anti-KIF22, anti-KIF4 (B), anti-phospho-H3S10 (C), and γ -H2AX (D). Cells were treated with 25 μ M etoposide for 1 h as a control for DNA damage. Dashed lines represent spindle axes. Bars, 10 μ m.

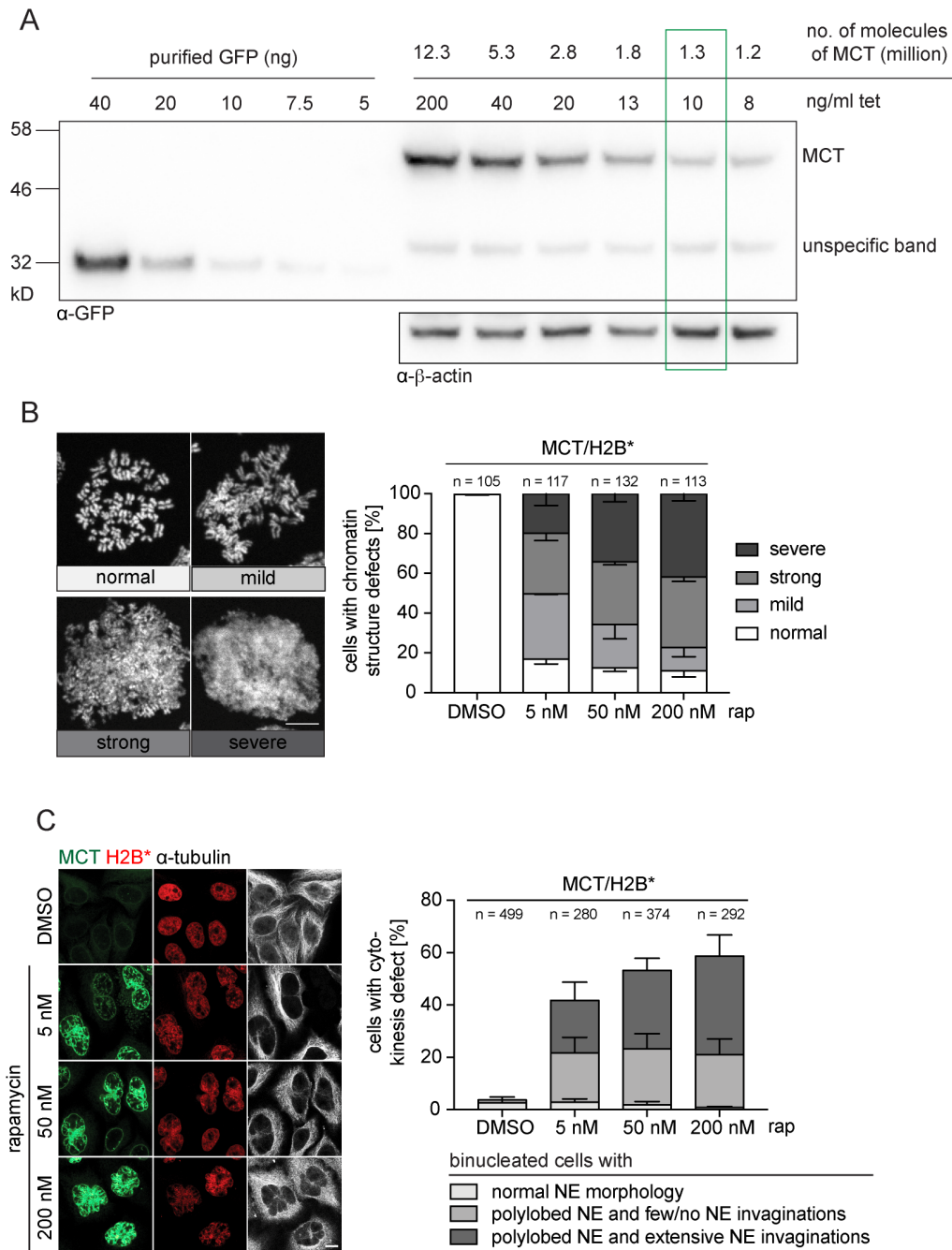


Figure S4. Expression of the MCT at a level similar to the endogenous INM protein LAP2 β causes chromatin condensation and cytokinesis defects. (A) MCT/H2B* cells were treated with the indicated concentrations of tetracycline (tet) for 16 h, harvested and total cell lysates analyzed by quantitative immunoblotting. Recombinant purified GFP served as a standard to estimate the number of MCT molecules. At a concentration of 10 ng/ml tet, the level of the MCT approximately corresponds to the level of endogenous LAP2 β (1.3×10^6 , Itzhak et al., 2016). (B) Experiment was performed as in Figure S1B, except that tetracycline was lowered to 10 ng/ml and rapamycin was used at the indicated concentrations. Structural defects observed in mitotic chromatin spreads upon expression of the MCT were classified into four categories as in Figure 4D. Quantification of each phenotype at indicated levels of rapamycin (N=3; mean \pm SEM; n: number of analyzed cells). (C) Synchronized MCT/H2B* cells were released from G1-S arrest and induced, as in Figure 1, but only with 10 ng/ml tetracycline and at the indicated concentrations of rapamycin. Cells were fixed 16 h later and analyzed by confocal microscopy. Binucleation and post-mitotic aberrations were quantified (N=3; mean \pm SEM; n: number of analyzed cells). Bars, 10 μ m.

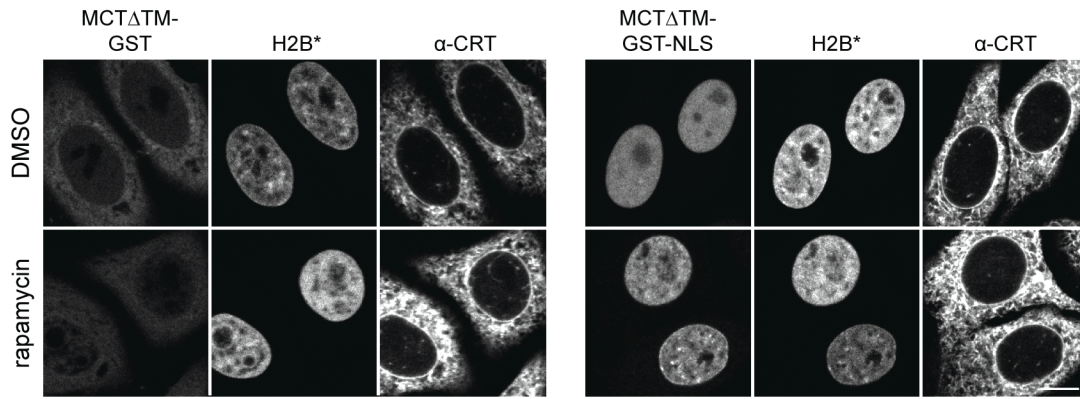


Figure S5. Localization of MCT Δ TM-GST and MCT Δ TM-GST-NLS in interphase cells. MCT Δ TM-GST(-NLS) cells were synchronized and treated with DMSO or 200 nM rapamycin for 2 h. Cells were fixed and imaged by confocal microscopy. Bar, 10 μ m.

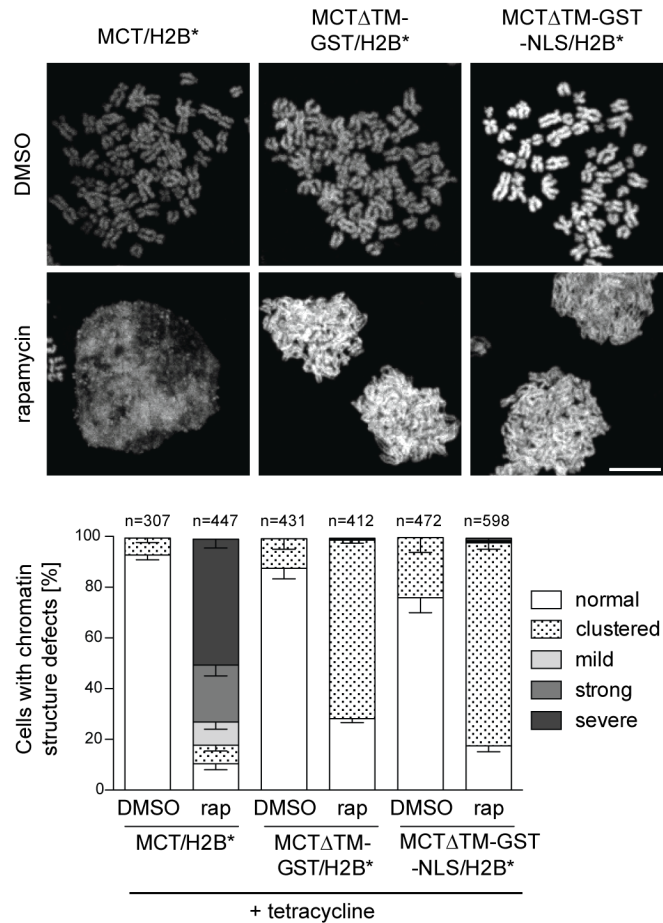


Figure S6. Comparison of mitotic chromatin organization for MCT/H2B*, MCT Δ TM-GST/H2B* or MCT Δ TM-GST-NLS/H2B* cells. Cells were synchronized and treated as for Figure 4D, except that tetracycline was added 16 h before release from the G1/S arrest. To obtain comparable GFP expression level, MCT/H2B* and MCT Δ TM-GST(-NLS)/H2B* cells were treated with 5 ng/ml and 10 ng/ml tetracycline, respectively. Representative images of mitotic chromatin spreads (upper panels). For quantification (below), spreads were classified into one of the five indicated categories. The category 'clustered' comprises spreads in which chromosomes display distinguishable arms but chromosomes remain in clear proximity in the spreads, as seen for MCT Δ TM-GST/H2B* or MCT Δ TM-GST-NLS/H2B* in presence of rapamycin. N=3; mean \pm SEM; n: total number of analyzed cells. Bar, 10 μ m.

Movie S1. Time lapse microscopy of rapamycin-treated MCT/H2B* cells.

Confocal time lapse microscopy of synchronized MCT/H2B* cells treated with 200 nM rapamycin before mitotic entry as in Figure 1D. Note that in this polyclonal MCT/H2B* cell line only about 70-80% of cells express the MCT. Bar: 10 μ m.

Supplemental reference

Itzhak, D.N., S. Tyanova, J. Cox, and G.H. Borner. 2016. Global, quantitative and dynamic mapping of protein subcellular localization. *Elife*. 5. doi:10.7554/eLife.16950